Bioorganic & Medicinal Chemistry 20 (2012) 270–278

Contents lists available at SciVerse ScienceDirect

Bioorganic & Medicinal Chemistry

journal homepage: www.elsevier.com/locate/bmc

NMR-based conformational analysis of sphingomyelin in bicelles

Toshiyuki Yamaguchi [a,b], Takashi Suzuki [a], Tomokazu Yasuda [a], Tohru Oishi [a,c], Nobuaki Matsumori [a,*], Michio Murata [a,b,*]

[a] Department of Chemistry, Graduate School of Science, Osaka University, Toyonaka, Osaka 560-0043, Japan
[b] JST, ERATO, Lipid Active Structure Project, Toyonaka, Osaka 560-0043, Japan
[c] Department of Chemistry, Graduate School of Sciences, Kyushu University, Higashi-ku, Fukuoka 812-8581, Japan

ARTICLE INFO

Article history:
Received 14 September 2011
Revised 31 October 2011
Accepted 1 November 2011
Available online 7 November 2011

Keywords:
Sphingomyelin
Bicelle
NMR spectroscopy
Lipid rafts
Conformation

ABSTRACT

Sphingomyelin (SM) is a common sphingolipid in mammalian membranes and is known to be substantially involved in cellular events such as the formation of lipid rafts. Despite its biological significance, conformation of SM in a membrane environment remains unclear because the noncrystalline property and anisotropic environment of lipid bilayers hampers the application of X-ray crystallography and NMR measurements. In this study, to elucidate the conformation of SM in membranes, we utilized bicelles as a substitute for a lipid bilayer membrane. First, we demonstrated through ^{31}P NMR, ^{2}H NMR, and dynamic light scattering experiments that SM forms both oriented and isotropic bicelles by changing the ratio of SM/dihexanoyl phosphatidylcholine. Then, we determined the conformation of SM in isotropic bicelles on the basis of coupling constants and NOE correlations in ^{1}H NMR and found that the C2–C6 and amide groups of SM take a relatively rigid conformation in bicelles.

1. Introduction

Until the late 1990s, plasma membranes were considered to be a two-dimensional fluid where lipids and proteins diffuse freely. During the last decade, their heterogeneity and complexity have been widely recognized; for example, it has been found that sphingomyelin (SM), the most abundant sphingolipid in biomembranes, forms microdomains called lipid rafts on a plasma membrane in the presence of cholesterol.[1] Lipid rafts are believed to play a key role in numerous cellular processes such as signal transduction, protein sorting, and cholesterol shuttling.[1,2] In addition, they are recognized as potential sites for toxin interactions, entryways for pathogens,[3] and fusion sites for HIV.[4–6] Despite such biological/pathological significance, the manner in which raft-forming lipids self-assemble to form a nanometer-scale organization is still unknown, largely because of the rapid association and dissociation equilibrium of lipid molecules in rafts. To gain a fundamental understanding of molecular interactions in lipid rafts, exploration of the structures and dynamics of SM in membrane environments is crucial.

So far, however, the conformation of SM in membrane environments has not been elucidated, although its conformation in organic solvents has been extensively analyzed on the basis of coupling constants by NMR experiments.[7,8] To mimic the membrane environment, micellar media such as sodium dodecyl sulfate are often used; however, as a membrane alternative, micelles are controversial because of their small radius, high curvature, and lack of lamellar structures. Recently, bicelles has been found to better reproduce a natural membrane environment since they possess true lipid bilayer portions.[9,10] Bicelles are generally comprised of a long-chain phospholipid such as dimyristoyl phosphatidylcholine

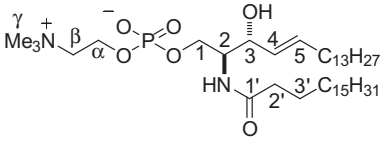

D-*erythro*-*N*-stearoyl-sphingomyelin
(SSM)

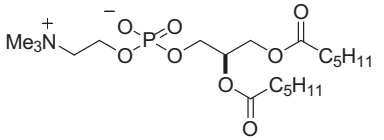

1,2-dihexanoyl-3-*sn*-phosphatidylcholine
(DHPC)

Figure 1. Structures of stearoylsphingomyelin (SSM) and dihexanoylphosphatidylcholine (DHPC).

* Corresponding authors. Address: Department of Chemistry, Graduate School of Science, Osaka University, Toyonaka, Osaka 560-0043, Japan. Tel.: +81 6 6850 5790; fax: +81 6 6850 5789 (N.M); tel./fax: +81 6 6850 5774 (M.M).

E-mail addresses: matsmori@chem.sci.osaka-u.ac.jp (N. Matsumori), murata@chem.sci.osaka-u.ac.jp (M. Murata).

0968-0896/$ - see front matter © 2011 Elsevier Ltd. All rights reserved.
doi:10.1016/j.bmc.2011.11.001

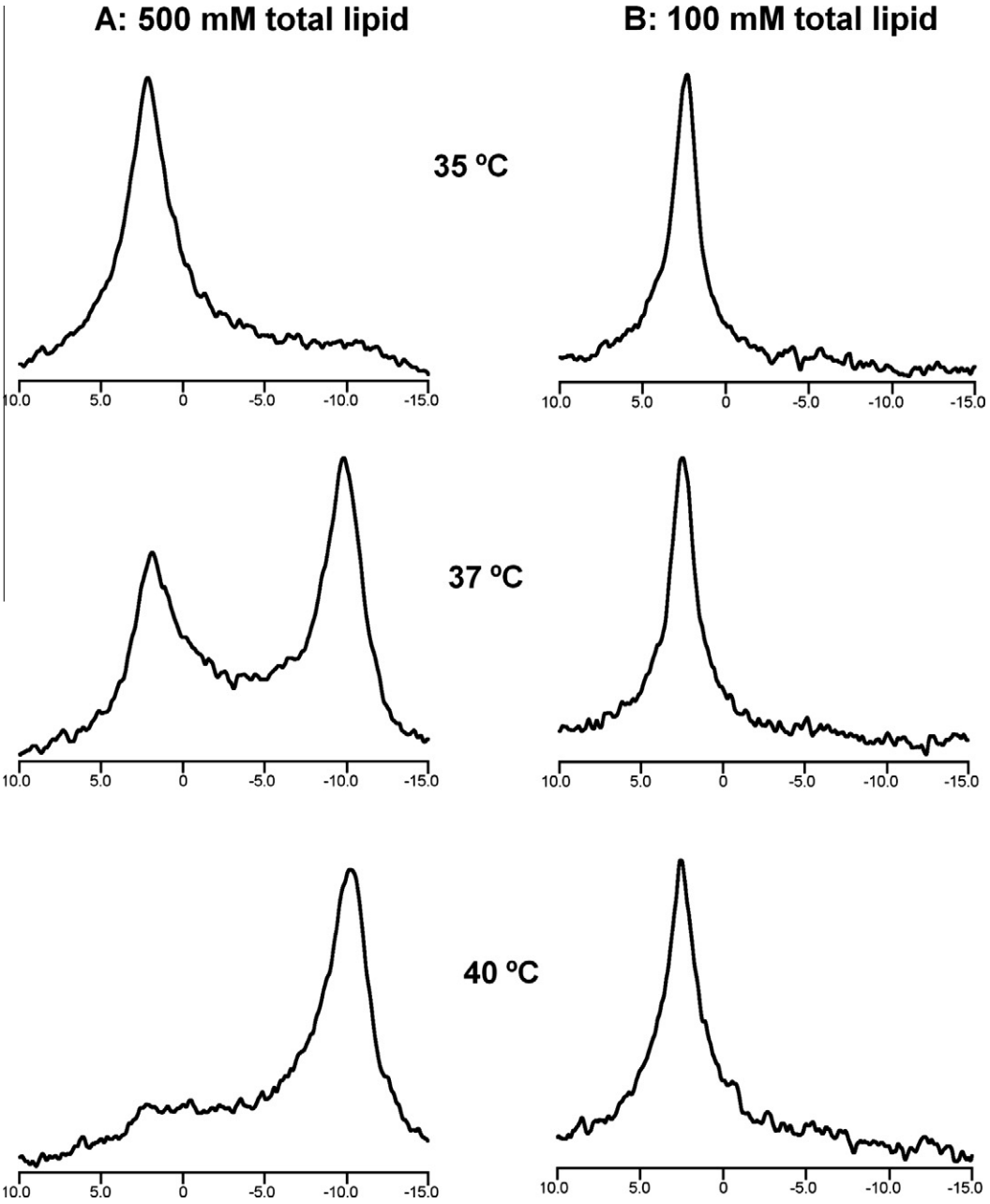

Figure 2. ^{31}P NMR spectra of bSM/DHPC (4:1) bicelles at 35, 37, and 40 °C. The total lipid concentration was 500 mM (A) and 100 mM (B).

(DMPC), and a short-chain one such as dihexanoyl phosphatidylcholine (DHPC, Fig. 1). The size and shape of bicelles can be controlled by the ratio of long-chain phosphatidylcholine (PC) to short-chain PC, that is, *q*. At higher *q* values, bicelles adopt a magnetically aligned lamellar bilayer morphology. In contrast, when the *q* values are decreased, bicelles become disk-shaped. In this configuration, the planar region consisting of long-chain lipids is surrounded by a rim comprised of short-chain lipids. Bicelles with the *q* value less than 1 undergo fast tumbling and can be regarded as isotropic in aqueous solutions, thus allowing high-resolution ^{1}H NMR measurements. In fact, small bicelles have often been used for structural determinations of small integral peptides and membrane-bound agents.[11–13]

In this study, we applied the bicelle technique to explain the structure of SM in a membrane environment. Since there have been no reports so far on bicelle formation with SM, we first demonstrated that SM forms both oriented and isotropic bicelles by changing the ratio of SM/DHPC. Then, the conformation of SM in isotropic bicelles was determined on the basis of vicinal ^{1}H–^{1}H coupling constants and NOEs. Although some NOESY cross peaks were completely overlapped, we successfully prepared a site-selectively deuterated SM and made the NOE assignment for the central portion of SM (C1–C5).

2. Results and discussion

2.1. Formation of oriented bicelles containing SM

Before dealing with the conformation of SM in bicelles, we examined whether SM forms bicelles with DHPC, as is the case with DMPC. ^{31}P NMR is generally used for characterizing the orientation and morphology of bicelles.[14] In oriented bicelles with the normal perpendicular to the direction of the magnetic field, ^{31}P NMR spectra show two signals. The high-field resonance is

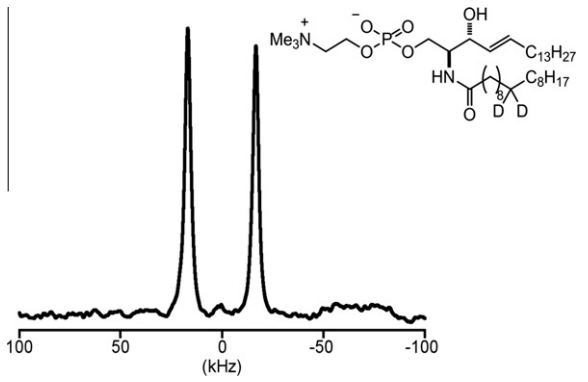

Figure 3. ^{2}H NMR spectrum of SSM/10′-d_2-SSM/DHPC (3:1) bicelle (500 mM) at 37 °C.

attributed to long-chain lipids in the planar section, whereas the downfield resonance is attributed to DHPC on the rim of the disks.[14] Since large quantities of SM are necessary for ^{31}P NMR experiments, we used bovine brain SM (bSM), which is a standard SM in biological and biophysical studies and contains about 50% stearoylsphingomyelin (SSM, Fig. 1).[15] We first examined the orientation of bicelles composed of bSM/DHPC (4:1, $q = 4$) at 500 mM of the total lipid concentration (bSM + DHPC). As shown in Figure 2A, ^{31}P NMR spectra showed two signals at 37 °C; high filed resonance is attributable to the planar part of oriented bicelles, and low-field one is due to the rim portion. This implies that bSM/DHPC bicelles are aligned along the external magnetic field; On the other hand, a broad isotropic signal observed at 35 °C indicates that magnetically aligned bicelles do not occur, and the spectral feature at 40 °C suggests possible vesicle formation (Fig. 2A). Bicelles with the same q value ($q = 4$) at 100 mM of the total lipid concentration showed no orientation at the tested temperatures (Fig. 2B). In separate experiments where the total lipid concentration was varied from 100 mM to 500 mM (Figs. S1–S5, Supplementary), we observed that bicelles are oriented at concentrations of more than 200 mM. These data show that alignment of bSM/DHPC bicelles is significantly influenced by not only temperature but also total lipid concentration; in particular, bSM/DHPC bicelles with $q = 4$ can be oriented in a narrow temperature range at around 37 °C.

To further confirm that SM/DHPC bicelles with $q = 4$ are magnetically oriented, we prepared a deuterated SSM (10′-d_2-SSM, Fig. 3) and measured ^{2}H NMR. Details of the preparation of 10′-d_2-SSM are given in the Supplementary. Fig. 3 depicts the ^{2}H NMR spectrum of 10′-d_2-SSM/DHPC bicelles ($q = 4$) at the total lipid concentration of 500 mM and shows a well-resolved doublet without any center peak. It is known that lipid molecules residing in the bilayer portion of oriented bicelles result in sharp doublet signals in the ^{2}H NMR spectrum, while those in the rim portion of oriented bicelles show peaks near the spectral center because of the isotropic nature of the rim portion.[16] Fig. 3 clearly demonstrates not only that SM/DHPC bicelles are magnetically aligned but also that SM molecules reside exclusively in the bilayer portions of bicelles. Although ^{2}H splitting of D_2O residing in hydration shell of oriented bicelles was sometimes used for evaluating the formation of oriented bicelles,[17] ^{2}H splitting of 10′-d_2-SSM unequivocally demonstrates the oriented bicelle formation because it resides in the bicelles.

We also measured ^{2}H NMR spectra of SSM/10′-d_2-SSM/DHPC (3:1) bicelles at various temperatures (Fig. S9, Supplementary), which unexpectedly suggest that aligned bicelles occur from 30 to 50 °C. This is different from Fig. 2A that indicates that the oriented bicelles forms only at around 37 °C. This discrepancy is probably caused by the difference of SM used; in Fig. 2 we used brain SM that is a mixture of SMs with various acyl-chain lengths as described earlier, but we used pure SSM in the ^{2}H NMR experiments. This suggests that oriented bicelles formed by pure SSM is more temperature-tolerant than those by brain SM. Based on this finding, we will try to prepare more stable oriented bicelles using pure SM, and the results will be reported in due course.

Next, to estimate the size of bSM/DHPC (4:1) bicelles, we carried out dynamic light scattering experiments by varying temperature and concentration (Fig. 4). All preparations basically showed a single main peak, thus indicating that SM and DHPC form aggregates of relatively uniform size; that is, coexistence of different-sized aggregates such as micelles and vesicles does not occur. For bicelles with $q = 4$ at 500 mM of the total lipid concentration, the bicelle size increased with increasing temperature from 35 to 40 °C (Fig. 4A). Taking account of the results of ^{31}P NMR experiments in Fig. 2A, which illustrate that 500 mM bicelles with $q = 4$ are magnetically aligned only at 37 °C, bicelles around 100 nm in diameter tend to be oriented, which is comparable to the size reported for aligned DMPC/DHPC bicelles.[18] The larger size at 40 °C (Fig. 4A) suggests the formation of vesicles, which is consistent with the spectral features of ^{31}P NMR in Fig. 2A. At the low lipid concentration (100 mM), bicelles with $q = 4$ become smaller

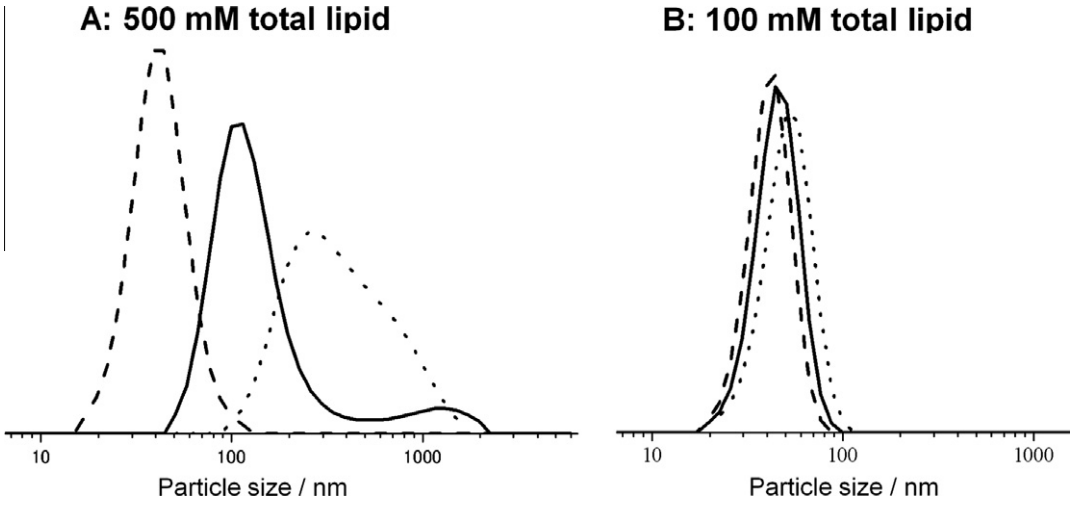

Figure 4. Dynamic light scattering results of bSM/DHPC bicelles with $q = 4$ at 35 °C (dashed line), 37 °C (solid line), and 40 °C (dotted line). Total lipid concentration was 500 mM (A) and 100 mM (B).

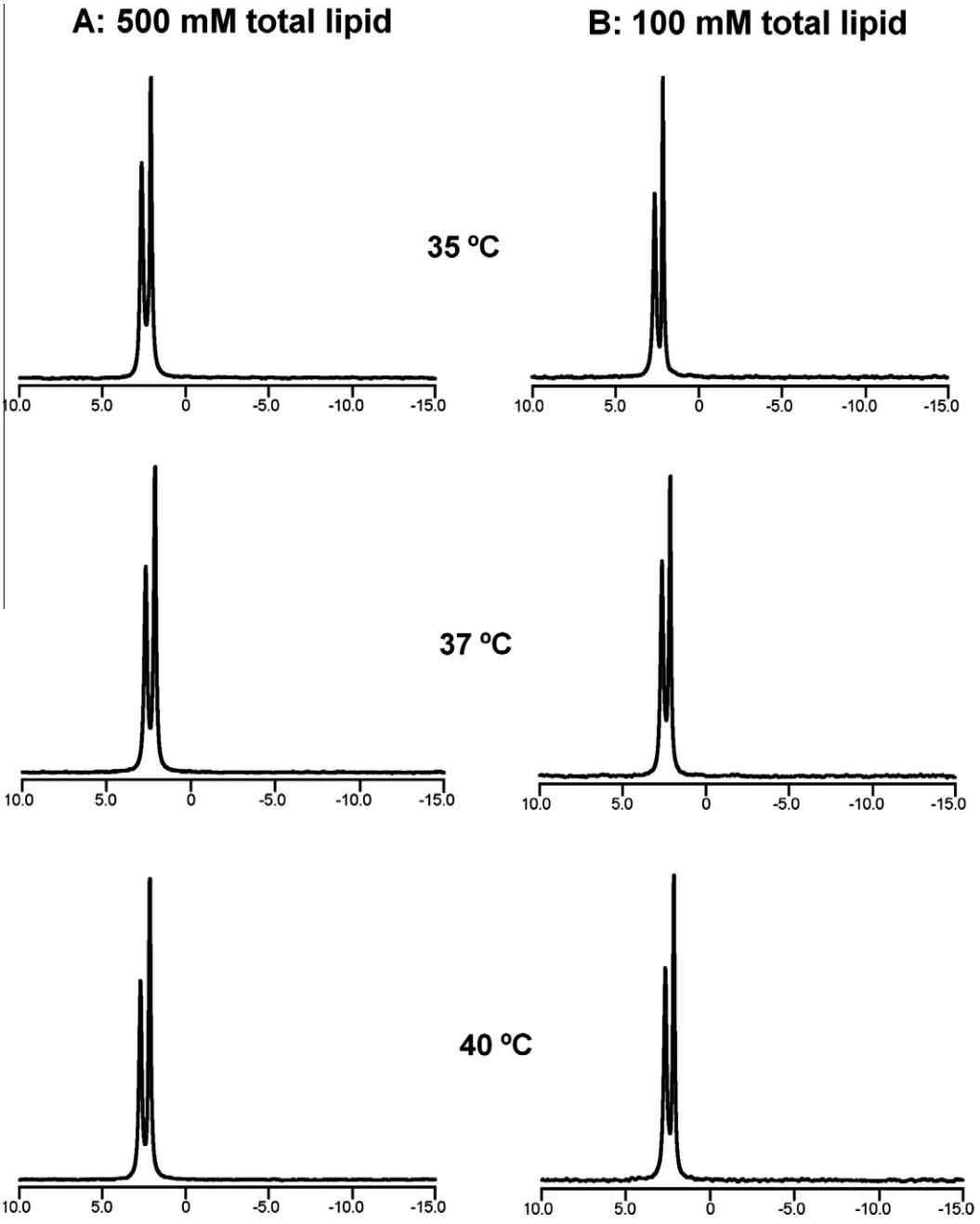

Figure 5. ^{31}P NMR spectra of bSM/DHPC = 1:2 bicelles at 35 °C, 37 °C, and 40 °C. The total lipid concentration was 500 mM (A) and 100 mM (B).

(Fig. 4B), which is also consistent with the isotropic orientation shown in the ^{31}P NMR experiments. These data indicate that the size of bicelles with $q = 4$ considerably depends not only on temperature but also on the concentration of lipids.

2.2. Formation of isotropic bicelles containing SM

After finding that SM forms oriented bicelles, we examined the formation of isotropic bicelles comprised of bSM/DHPC (1:2, $q = 0.5$). In the ^{31}P NMR spectra, two sharp signals in close vicinity ($\delta_{SM} = 2.7$ ppm, $\delta_{DHPC} = 2.1$ ppm) are clearly observed (Fig. 5), thus indicating the formation of small and magnetically isotropic bicelles. The low-field resonance of the ^{31}P signal of SM is probably attributable to intramolecular hydrogen bonding, which is not present in phosphatidylcholine.[19,20] As depicted in Figure 5, ^{31}P NMR signals of $q = 0.5$ bicelles are virtually unaffected by temperature (35–40 °C) or lipid concentration (100–500 mM).

Dynamic light scattering experiments also showed that the size of bSM/DHPC bicelles with $q = 0.5$ is virtually unaffected by temperature or concentration (Fig. 6), which is consistent with the results of ^{31}P NMR experiments (Fig. 5). The size of bicelles with $q = 0.5$ is around 20 nm in diameter, which is comparable to that of isotropic DMPC/DHPC bicelles (Fig. S6, Supplementary). These results suggest that an SM/DHPC system with $q = 0.5$ forms stable isotropic bicelles at broad temperature and concentration ranges.

Thus, in the following conformation analysis of SM in isotropic bicelles, we used SM/DHPC (1:2) bicelles with total lipid concentration of 100 mM and measured NMR spectra at 37 °C.

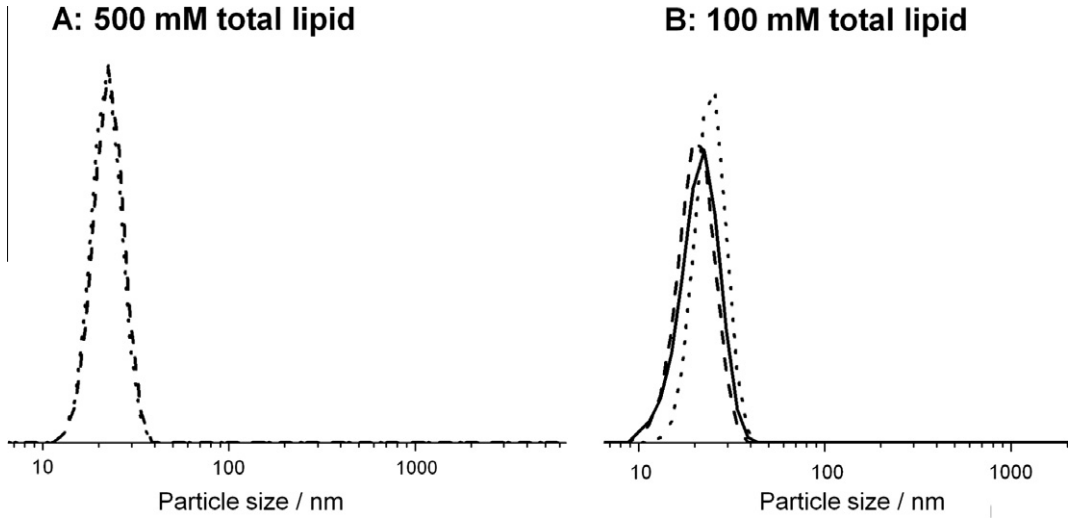

Figure 6. Dynamic light scattering of bSM/DHPC bicelles with q = 0.5 at 35 °C (dashed line), 37 °C (solid line), and 40 °C (dotted line). Total lipid concentration was 500 mM (A) and 100 mM (B).

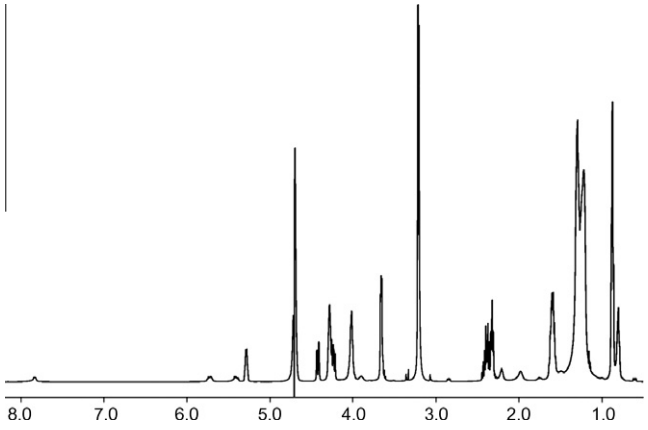

Figure 7. Five hundred megahertz ^{1}H NMR spectrum of SSM/DHPC (1:2) bicelles at 37 °C in H_2O/D_2O (9:1). Total lipid concentration was 100 mM.

Table 1
^{1}H chemical shifts (ppm) of SSM in SSM/DHPC (1:2) bicelles at 37 °C

Position	δ^a	Position	δ^a
NH	7.83	Hβ	3.66
H5	5.72	Hγ	3.20
H4	5.41	H2'	2.21
Hα	4.28	H6	1.98
H1	4.02	H3'	1.60
H3	4.02	CH_2	1.22
H2	3.90	H18,18'	0.80

[a] Chemical shifts were referenced to DSS.

Table 2
$^3J_{H/H}$ values of SSM in bicelles and in methanol

	$^3J_{H2/H3}$ (Hz)	$^3J_{H3/H4}$ (Hz)	$^3J_{H2/NH}$ (Hz)
In SSM/DHPC (1/2) bicelles	10.7	7.7	9.1
In CD_3OD	8.4	7.6	—[a]

[a] Coupling constant was not observed because of exchanging N–H with N–D.

2.3. Measurements of ^{1}H NMR of SSM-DHPC isotropic bicelles

For the following ^{1}H NMR measurements, we used SSM (Fig. 1) that was purified by HPLC from bovine bSM. The ^{1}H NMR spectrum shown in Fig. 7 was measured with SSM/DHPC bicelles (1:2, 100 mM of the total lipid concentration) in H_2O/D_2O (9:1, v/v) at 37 °C. Although DHPC gave much stronger signals, resonances from SSM are relatively well resolved and successfully assigned (Table 1). One-dimensional and E.COSY spectra were recorded to determine relevant $^3J_{H/H}$ values (Table 2). A large $^3J_{H\text{-}2/H\text{-}3}$ value indicates that the C2–C3 bond largely takes an anti-conformation.[21] As compared to the $^3J_{H,H}$ data in CD_3OD (Table 2), the $^3J_{H\text{-}2/H\text{-}3}$ value in bicelles was shown to be larger than that in CD_3OD, indicating that anti-conformation is more predominant for the C2–C3 bond in bicelles than in CD_3OD. Similarly, judging from a reported Karplus relation for $^3J_{HN/C\alpha H}$ of peptides,[22] the observed $^3J_{H2/NH}$ (9.1 Hz) implies a major anti-rotamer for the C2–N bond. Rotamer around the C3–C4 bond will be discussed later.

To obtain H–H distance information of SSM, NOESY experiments were carried out for SSM/DHPC (1:2) bicelles (Fig. 8A). We successfully observed conformationally relevant NOEs such as H-3/H-5 and H-2/H-4 (Fig. 8A). The amide proton (7.83 ppm) also gave an NOE cross peak at around 4 ppm corresponding to H-1 and H-3 resonances (Fig. 8B); however, it was difficult to assign the cross peak because of the complete overlapping of H-1 and H-3 signals. Because the unambiguous assignment of the NOE is necessary to determine the conformation around the amide portion, we synthesized 3-*d*-SSM to deplete the overlapping H-3 signal. The synthesis of 3-*d*-SSM is shown in Scheme 1, which is a slight modification of a previous report.[23] In short, starting from L-serine, deuterium was introduced by the reduction of ketone with $LiAlD_4$, and then olefin metathesis by the Grubbs catalyst, followed by the introduction of a choline group and an acyl chain, furnishing 3-*d*-SSM with 100% deuterium labeling rate. The NOESY measurement in isotropic bicelles containing 3-*d*-SSM showed that the cross peak intensity of concern was significantly weakened (Fig. 8C); the evaluation of the cross-peak intensity showed that the cross-peak volume in Fig. 8C is reduced to 49% of that in Fig. 8B. This means that the correlations for amide-H/H-1 and amide-H/H-3 contribute equally to the cross-peak in Fig. 8B.

2.4. Conformation of SSM in bicelles

As described above, the large $^3J_{H\text{-}2/H\text{-}3}$ (10.7 Hz, Table 2) in bicelles indicates the anti-conformation for the C2–C3 bond.[21] Likewise, judging from the empirical Karplus relation between

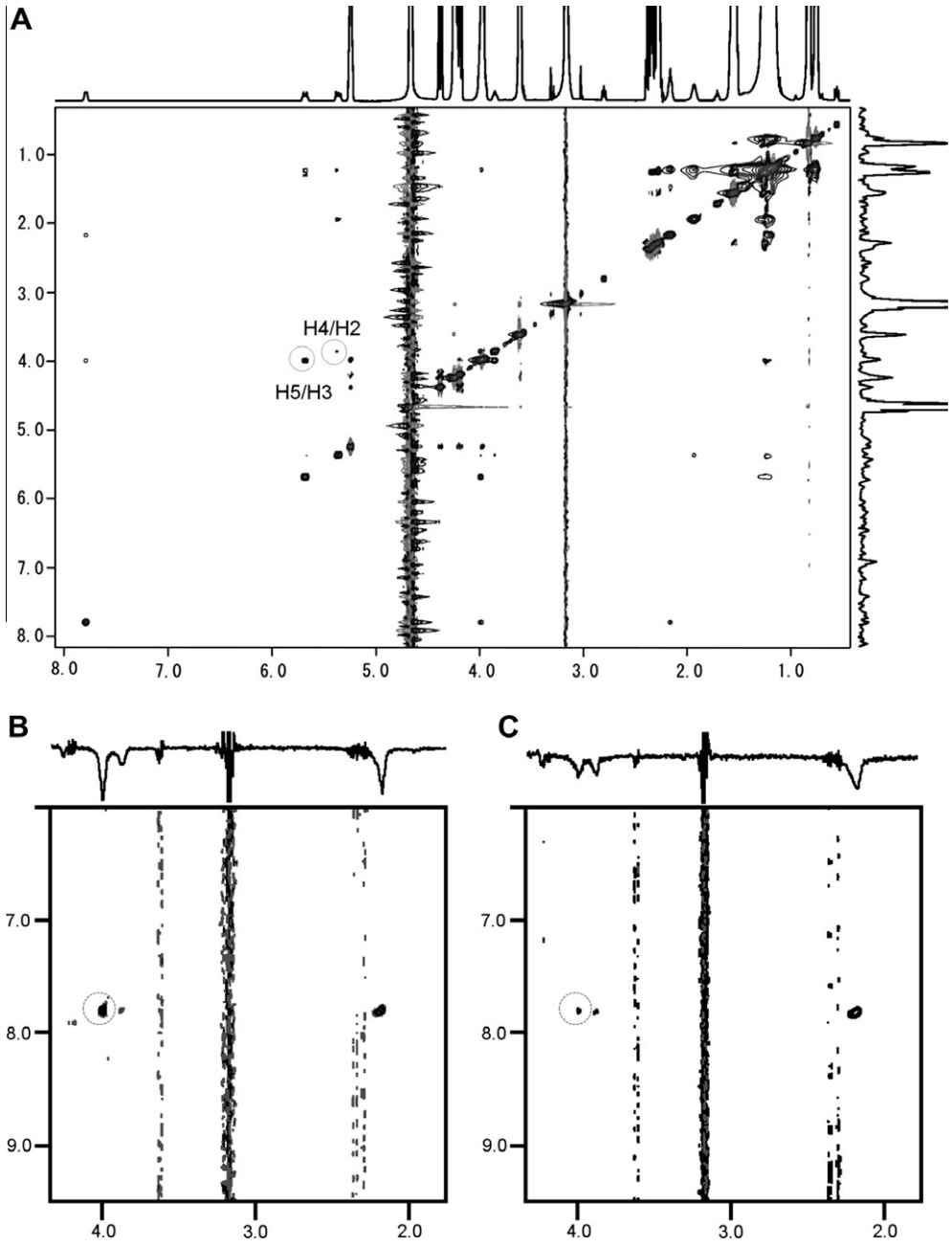

Figure 8. NOESY spectrum of SSM/DHPC (1:2) bicelles at 37 °C in H_2O/D_2O (9:1) (A) and its expanded spectrum (B). Expanded NOESY spectrum of 3-*d*-SSM/DHPC (1:2) bicelles (C). The total lipid concentration was 100 mM in all spectra. The cross peak in the dashed circle in spectrum (B) is markedly weakened in spectrum (C), indicating that the cross peak is mostly attributable to the NOE arising from the amide and H3.

amide protons and Cα protons in peptides,[22] the observed $J_{NH/H\text{-}2}$ (9.1 Hz, Table 2) also implies that H-2/NH takes an anti-orientation.

On the other hand, to our knowledge, Karplus relation for $C(sp^2)$–$C(sp^3)$ bonds has not been reported so far, probably because of the scarce occurrence of such bonds in peptides and proteins. Although the parameters required to define a Karplus relation are traditionally determined using coupling constants of molecules with known geometries,[24] it is now feasible to calculate coupling constants using quantum-chemistry methods for any arbitrary geometry. Recently, it has been shown that the density function theory can calculate scalar couplings with reasonable accuracy[25,26]; hence, to derive a Karplus relation of the C3–C4 bond of SSM, we calculated scalar coupling constants of the bond by B3LYP/6-31G(d,p) basis set.[27] A truncated structure of SM (Fig. S8, Supplementary) was used for the calculation, and the C3–C4 bond was rotated through 360° in 30° increments. At each point, geometry optimization was performed with the rotation of C3–C4 bond fixed and then the coupling constant was calculated. The Karplus relation (Fig. S8, Supplementary) was derived by fitting the resultant coupling constants to a general Karplus equation. The observed $^3J_{H\text{-}3/H\text{-}4}$ value for the C3–C4 bond (7.7 Hz, dashed line in Fig. S8, Supplementary) revealed that anti-orientation for H-3/H-4 was predominant, which was further supported by the NOE observed for H-3/H-5.

We then constructed a possible conformation of SM partial structure (C1–C6 and amide portions) by considering the dihedral angles as well as the NOEs obtained for NH/H-3, H-2/H-4,

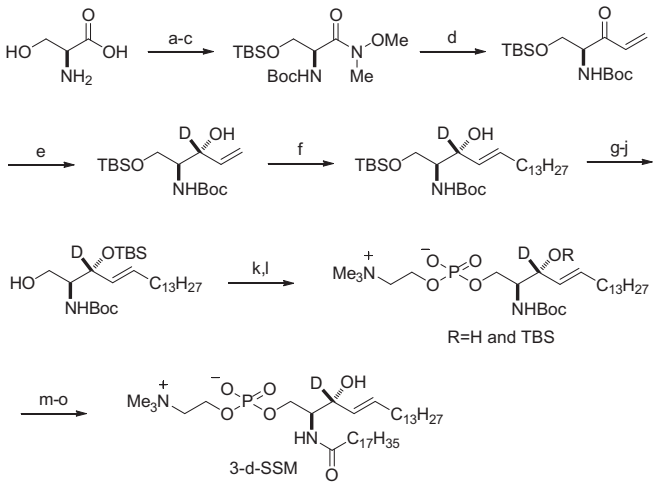

Scheme 1. Synthesis of 3-*d*-SSM. Reagents and Conditions: (a) $(Boc)_2O$, NaOH, H_2O, dioxane, rt,6 h; (b) NH(Me)OMe·HCl, NMM, EDC, CH_2Cl_2, −15 °C, 2 h; (c) TBSCl, imidazole, DMF, rt, 1 h (74% for three steps); (d) vinyl MgBr, THF, rt, 1.5 h (91%); (e) $LiAlD_4$, THF, rt, 40 min (15%); (f) 1-pentadecene, Grubbs II catalyst, *p*-quinone, CH_2Cl_2, 55 °C, 1.5 h (60%); (g)TBAF, THF, rt, 25 min (96%); (h) PivCl, pyridine, −30 °C, 2.5 h (92%); (i) TBSOTf, 2,6-lutidine, CH_2Cl_2, 0 °C, 30 min; (j) DBU, MeOH, rt, 14 h (57% for two steps); (k) 2-chloro-1,3,2-dioxaphosphoran-2-oxide, Et_3N, DMAP, benzene, 0 °C, 1 h; (l) Me_3N, CH_3CN, 85 °C, 72 h (61% for two steps); (m) TFA, CH_2Cl_2, 0 °C, 30 min (n) *p*-nitrophenyl octadecanoate, Et_3N, DMAP, THF, rt, 13 h (o) TBAF, THF, rt, 26 h (54% for three steps).

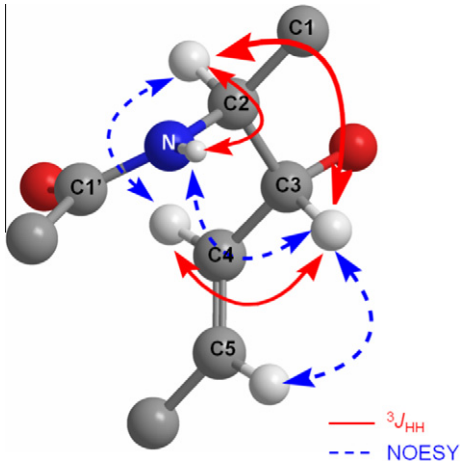

Figure 9. Conformation of the central part of SM in bicelles deduced from ^1H NMR data.

and H-3/H-5. The observed $^3J_{H,H}$ values typical for anti-orientation suggest that the conformational alteration hardly occurs with respect to these bonds. This is supported by the fact that the NOE data are completely consistent with the dihedral angles. Finally, energy minimization of the initial structure eventually resulted in the conformation of SM in bicelles, as shown in Fig. 9. Thus, we successfully determined the conformation of the partial structure of SM in bicelles and found that the C2–C6 and amide portions of SM take a relatively rigid conformation under membrane environments.

3. Conclusions

In this study, we demonstrated for the first time that SM and DHPC form both oriented and isotropic bicelles, and in particular, isotropic bicelles are found to be relatively tolerant to concentration and temperature changes. Then, using isotropic bicelles, we successfully elucidated the partial conformation of SM in a membrane environment on the basis of ^1H–^1H spin coupling constants and NOE data. To achieve this, it was necessary to synthesize 3-*d*-SSM to discriminate the overlapping signals in the NOESY spectrum as well as to establish the calculated Karplus equation for the C(sp^2)–C(sp^3) bond to obtain dihedral information for the C3–C4 bond of SM.

As described earlier, lipid rafts have attracted much attention because of their crucial roles in biological processes. However, the mechanism of raft formation, in particular the origin of molecular interactions in lipid rafts, remains elusive. The conformation of SM in a membrane environment is, therefore, indispensable for understanding the mode of molecular interactions that occur in lipid rafts and will provide a valuable insight into the mechanism of raft formation. For instance, one may notice that this conformational feature of SM facilitates intermolecular hydrogen bonds between SM amide groups, which may lead to stronger molecular interaction in SM membranes than PC membranes. NMR studies in this direction are currently underway in our group. In addition, with the bicelles comprised of SM available, it would become feasible to evaluate the influences of cholesterol on an SM-based membrane.

4. Experimental

4.1. Materials

Sphingomyelin (bovine, brain) and 1,2-dihexanoyl-3-*sn*-phosphatidylcholine (DHPC) were purchased from Avanti Polar Lipids (Alabaster, AL). Deuterium oxide was purchased from Euriso-top, and deuterium-depleted water was from ISOTEC. All other chemicals were obtained from standard venders. Thin-layer chromatography (TLC) was performed on a glass plate precoated with silica gel (Merck Kieselgel 60 F254).

4.2. Purification of SSM

Because commercially available semi-synthetic D-*erythro*-*N*-stearoyl-sphingomyelin (SSM) is a mixture of epimers at C3 of sphingosine, we purified SSM from bovine brain SM (Avanti polar lipid) by HPLC with a slightly modified procedure of the previous report.[28] Bovine brain SM was a mixture of SMs with 16:0 (2%), 18:0 (SSM, 49%), 20:0 (5%), 22:0 (8%), 24:0 (6%) and 24:1 (20%),[15] which were separated by reverse-phase HPLC (Shimadzu LC-10ADvp with an SPDM10Av photodiode array detector) with the following conditions; column: cosmosil-5C_{18}-AR-II (20 × 250 mm), eluent: MeOH, flow rate: 4 mL/min, detection: 205 nm UV absorption. Retention times are 55 min for C18:0-SM (SSM), 72 min for C20:0 and 90 min for C24:1.

4.3. Bicelle preparation

Bicelles were prepared according to a general procedure.[13,29] For ^{31}P NMR measurements and dynamic light scattering experiments, commercially available brain SM (bSM) was used without purification. bSM (ca. 220 mg for $q = 4$ bicelles or 90 mg for $q = 0.5$ bicelles) was dissolved in chloroform/methanol, dried in vacuo overnight, rehydrated with H_2O (600 μL for $q = 4$ bicelles or 245 μL for $q = 0.5$ bicelles), and vortexed vigorously. To the suspension was added DHPC in D_2O (0.5 M, 150 μl for $q = 4$ or 495 μL for $q = 0.5$) and the mixture was subjected to heating (60 °C) and cooling (0 °C) cycles and vigorous vortexing until becoming transparent. The total lipid concentration (bSM + DHPC) was 500 mM for both $q = 4$ and 0.5 bicelles. After both ^{31}P NMR and dynamic light scattering experiments were completed, the lipid solutions were

diluted to 100 mM by adding H_2O, and ^{31}P NMR and dynamic light scattering experiments were carried out again.

For ^2H NMR measurements,10′-d_2-SSM (4.8 mg, 6.5 μmol) and purified SSM (14.5 mg, 19.8 μmol) were dissolved in methanol, dried in vacuo overnight, and mixed with DHPC (6.6 μmol) in H_2O (13.2 μL). To the mixture was added H_2O (200 μl), and the resultant suspension was vortexed vigorously until becoming transparent, lyophilized, and rehydrated with deuterium-depleted water (57 μL). The final concentration of lipid (SSM + DHPC) was 500 mM.

For ^1H NMR measurements, purified SSM (10.3 mg, 14.1 μmol) was dissolved in methanol, dried in vacuo overnight, and mixed with DHPC (28.2 μmol) in D_2O (282 μL). The mixture was vortexed vigorously until becoming transparent, lyophilized, and rehydrated with H_2O and D_2O (380 and 42 μL, respectively). The final concentration of lipid (SSM + DHPC) was 100 mM.

4.4. NMR measurements

^1H and ^{31}P NMR spectra were obtained on a JEOL ECA-500 (500 MHz) spectrometer. $^3J_{H/H}$ values were extracted from 1D ^1H NMR and 2D exclusive COSY (E.COSY) spectra.[30–32] ^1H chemical shifts were referenced to 3-(trimethylsilyl)-1-propanesulfonic acid sodium salt (DSS). The digital resolution for the 1D ^1H NMR spectrum was 0.076 Hz/point. The FID data of E.COSY experiment were acquired with 24 scans per inclement of 4096 (F2) × 256 (F1) matrix and processed with 2 and 4 times zero-filling for F1 and F2, respectively. To extract spin coupling constants from the E.COSY spectrum, a final digital resolution of 0.076 Hz/point in F2 was achieved by inverse Fourier transformation, 8 times zero-filling, and back transformation of selected traces. NOESY experiments were acquired with 12 scans per inclement of 2048 (F2) × 256 (F1) matrix and with 30 ms of mixing time. All the 1D and 2D ^1H spectra were recorded at 37 °C.

^{31}P NMR spectra were acquired with a digital resolution of 4.9 Hz/point. ^{31}P chemical shifts were referenced to 85% phosphoric acid. An exponential line broadening of 25 Hz was applied to the FID before Fourier transformation for both the oriented and isotropic bicelles.

^2H NMR experiments were carried out on a JEOL ECA-400 (400 MHz) spectrometer. ^2H NMR spectra were recorded at 61.4 MHz using a standard quadrupole-echo pulse sequence.[33] The 90° pulse width was 0.1 μs, interpulse delay was 30 μs, acquisition time was 16.38 ms, and recycle delay was 0.5 s. The sweep width was 500 kHz, and delay between the second 90° pulse and data acquisition was 20 μs. The number of scans was 24000. An exponential line broadening of 1000 Hz was applied to the FID before Fourier transformation.

4.5. Dynamic light scattering

The sizes of bicelles were evaluated by dynamic light scattering at 20–50 °C. The concentration of bicelles was 500 or 100 mM. All histograms were obtained on a HORIBA LB-550 dynamic light scattering particle size analyzer.

4.6. Dihedral angle analysis using $^3J_{H/H}$

In this study, dihedral angles for three bonds in SM, C2–C3, C3–C4, and C2–N, were analyzed using $^3J_{H/H}$ values. Reported Karplus relations were adopted for the rotations of the C2–C3[21] and C2–N[22] bonds. On the other hand, because no Karplus type equation has been reported for C(sp^2)–C(sp^3) bond, Karplus relation for the C3–C4 bond was derived from spin coupling constants calculated by GIAO method on the Gaussian 09W software.[34] A truncated model including the interfacial region of SM (as shown in Fig. S8, Supplementary) was used for calculating $^3J_{H3/H4}$ of SM. The C3–C4 bond was rotated through 360° in 30° degree increments, and at each point structure was optimized at the B3LYP/6-31G(d,p) level of theory with the C3–C4 bond rotation fixed. Spin–spin coupling constants were calculated with GIAO method using B3LYP/6-31G(d,p) basis set.[27] The resultant coupling constants were fitted to a general Karplus Eq. (1) with a dihedral angle (θ) and a parameter (ϕ) that reflects the phase shift between the cosine modulation and the dihedral angle.

$$^3J_{H/H} = A\cos^2(\theta+\phi) + B\cos(\theta+\phi) + C \quad (1)$$

The curve fitting was carried out using Origin 6.1 software. The resultant parameters in Eq. (1) are A = 6.95 Hz, B = −0.34 Hz, C = 1.84 Hz, and ϕ = 4.78° (Fig. S8, Supplementary).

4.7. Structure calculation

The initial partial structure of SM was constructed based on NOE and coupling constant data. The structure was minimized using MMFFs force field in MacroModel version 8.6.

Acknowledgments

We are grateful to Dr. Yuichi Umegawa and Mr. Mototsugu Doi, Osaka University, for their help in NMR measurements. This work was supported by Grant-In-Aids for JSPS Fellows, for Scientific Research (B) (No. 20310132) and (S) (No. 18101010), and by SUNBOR grant from Suntory Institute for Bioorganic Research, Japan. T.Y. expresses special thanks for the Global Center of Excellence (COE) Program 'Global Education and Research Center for Bio-Environmental Chemistry' of Osaka University.

Supplementary data

Supplementary data associated with this article can be found, in the online version, at doi:10.1016/j.bmc.2011.11.001.

References and notes

1. Simons, K.; Ikonen, E. *Nature* **1997**, *387*, 569.
2. Anderson, R. G. W.; Jacobson, K. *Science* **2002**, *296*, 1821.
3. van der Goot, F. G.; Harder, T. *Semin. Immunol.* **2001**, *13*, 89.
4. Liao, Z.; Cimakasky, L. M.; Hampton, R.; Nguyen, D. H.; Hildreth, J. E. K. *AIDS Res. Hum. Retrov.* **2001**, *17*, 1009.
5. Mañes, S.; del Real, G.; Lacalle, R. A.; Lucas, P.; Gómez-Moutón, C.; Sánchez-Palomino, S.; Delgado, R.; Alcamí, J.; Mira, E.; Martínez-A, C. *EMBO Rep.* **2000**, *1*, 190.
6. Puri, A.; Hug, P.; Jernigan, K.; Barchi, J.; Kim, H.-Y.; Hamilton, J.; Wiels, J.; Murray, G. J.; Blumenthal, R. *Proc. Natl. Acad. Sci. U.S.A.* **1998**, *95*, 14435.
7. Bruzik, K. S. *Biochim. Biophys. Acta* **1988**, *939*, 315.
8. Talbott, C. M.; Vorobyov, I.; Borchman, D.; Taylor, K. G.; DuPré, D. B.; Yappert, M. C. *Biochim. Biophys. Acta* **2000**, *1467*, 326.
9. Sanders, C. R.; Hare, B. J.; Howard, K. P.; Prestegard, J. H. *Prog. Nucl. Magn. Reson. Spectrosc.* **1994**, *26*, 421.
10. Sasaki, H.; Araki, M.; Fukuzawa, S.; Tachibana, K. *Bioorg. Med. Chem. Lett.* **2003**, *13*, 3583.
11. Dürr, U. H. N.; Yamamoto, K.; Im, S.-C.; Waskell, L.; Ramamoorthy, A. *J. Am. Chem. Soc.* **2007**, *129*, 6670.
12. Matsumori, N.; Morooka, A.; Murata, M. *J. Am. Chem. Soc.* **2007**, *129*, 14989.
13. Matsumori, N.; Murata, M. *Nat. Prod. Rep.* **2010**, *27*, 1480.
14. Loudet, C.; Manet, S.; Gineste, S.; Oda, R.; Achard, M.-F.; Dufourc, E. J. *Biophys. J.* **2007**, *92*, 3949.
15. Frazier, M. L.; Wright, J. R.; Pokorny, A.; Almeida, P. F. F. *Biophys. J.* **2007**, *92*, 2422.
16. Uddin, M. N.; Morrow, M. R. *Langmuir* **2010**, *26*, 12104.
17. Ottiger, M.; Bax, A. *J. Biomol. NMR* **1998**, *12*, 361.
18. Sasaki, H.; Fukuzawa, S.; Kikuchi, J.; Yokoyama, S.; Hirota, H.; Tachibana, K. *Langmuir* **2003**, *19*, 9841.
19. Schmidt, C. F.; Barenholz, Y.; Thompson, T. E. *Biochemistry* **1977**, *16*, 2649.
20. Henderson, T. O.; Glonek, T.; Myers, T. C. *Biochemistry* **1974**, *13*, 623.
21. Haasnoot, C. A. G.; De Leeuw, F. A. A. M.; Altona, C. *Tetrahedron* **1980**, *36*, 2783.
22. (a) Wang, A. C.; Bax, A. *J. Am. Chem. Soc.* **1996**, *118*, 2483; (b) Dreef, C. E.; Elie, C. J. J.; Hoogerhout, P.; van der Marel, G. A.; van Boom, J. H. *Tetrahedron Lett.* **1988**, *29*, 6513.

23. Yamamoto, T.; Hasegawa, H.; Hakogi, T.; Katsumura, S. *Org. Lett.* **2006**, *8*, 5569.
24. Bystrov, V. F. *Prog. Nucl. Magn. Reson. Spectrosc.* **1976**, *10*, 41.
25. Deng, W.; Cheeseman, J. R.; Frisch, M. J. *J. Chem. Theory Comput.* **2006**, *2*, 1028.
26. Lutnæs, O. B.; Ruden, T. A.; Helgaker, T. *Magn. Reson. Chem.* **2004**, *42*, 117.
27. Lee, C.; Yang, W.; Parr, R. G. *Phys. Rev. B* **1988**, *37*, 785.
28. Jungalwala, F. B.; Hayssen, V.; Pasquini, J. M.; McCluer, R. H. *J. Lipid Res.* **1979**, *20*, 579.
29. Mäler, L.; Gräslund, A. *Methods Mol. Biol.* **2009**, *480*, 129.
30. Griesinger, C.; Sørensen, O. W.; Ernst, R. R. *J. Am. Chem. Soc* **1985**, *107*, 6394.
31. Griesinger, C.; Sørensen, O. W.; Ernst, R. R. *J. Chem. Phys.* **1986**, *85*, 6837.
32. Griesinger, C.; Sørensen, O. W.; Ernst, R. R. *J. Magn. Reson.* **1987**, *75*, 474.
33. Davis, J. H.; Jeffrey, K. R.; Bloom, M.; Valic, M. I.; Higgs, T. P. *Chem. Phys. Lett.* **1976**, *42*, 390.
34. Frisch, M. J. et al. Gaussian 09, Revision A.02, Gaussian, Inc., Wallingford CT, 2009.